The Ion Chemistry in Hydrothermal Supercritical Aqueous Sodium Chloride Fluid Ablated From a Liquid Surface

W. Lowell Morgan, *Member, IEEE*

***Abstract*—Recent experiments and analyses have demonstrated the possibility of producing supercritical water at high temperatures and densities using a short-pulse electric surface discharge in saline solutions. This article describes a minimal ion chemistry model for supercritical salt water and the kinetics and thermodynamics of the chemistry. Time-dependent shock front calculations using the 1-D Zel'dovich–von Neumann–Doering theory are then presented. These demonstrate the feasibility of deflagration or even detonation fronts being produced by the rapid exothermic ion chemistry in the supercritical water. Finally, some potential applications to the treatment of wastewater with energy cogeneration are discussed.**

***Index Terms*—Deflagration, detonation, electric discharge, electrolyte, high pressure, high temperature, shock wave, supercritical water.**

I. Background

MORGAN and Rosocha [1] have recently published the results of experiments involving the discharge of a capacitor charged to high voltage across the surface of a saltwater solution. The electrical conductivity of an electrolyte is far greater at the liquid surface than the bulk conductivity. A short-pulse (tens to hundreds of nanoseconds) high-voltage-and-current surface discharge will then ablate liquid layers, much like laser ablation, driving the ablated fluid to supercritical temperatures, pressures, and densities above the saturation line, as is found with exploding wires in water. The experiments, theory, and applications are discussed herein.

The time scales involved were tens of nanoseconds to several microseconds. The geometry of the experiment is shown in Fig. 1. We detected Mach 4–8 shock fronts and near-sonic bulk fluid flow in the closed test reactor. The 15–20 J of electrical energy deposited was too small to produce such shocks. Similar observations were made by other authors in work published between 1985 and 2001. Their publications are cited in detail in [1].

As we have discussed in [1], the capacitive discharges involving small volumes of salt water that have been published over the past quarter century have involved one or another of two time scales. They have been either on the millisecond time scale producing the so-called plasmoids or spheroids of luminous gas or plasma above the liquid surface lasting for milliseconds. We have discussed these in some detail in [1] and [2]. The second time scale is what I am addressing here. These are discharges involving time scales of $\sim$10 ns to a microsecond or two. Whereas the plasmoids are created in times greater than the hydrodynamic time scale for plasmas at the water–air interface, in this work, I am discussing the physics of such discharges occurring on time scales much shorter than the hydrodynamic. The phenomena are quite different. The Internet is rife with videos of amateur experiments performed on the millisecond time scale with the claim that they observe "burning salt water." Most likely, they are merely observing Na(3P $\rightarrow$ 3S) radiation that has been trapped in the hot gas and plasma and escapes on the tens-of-millisecond time scale.

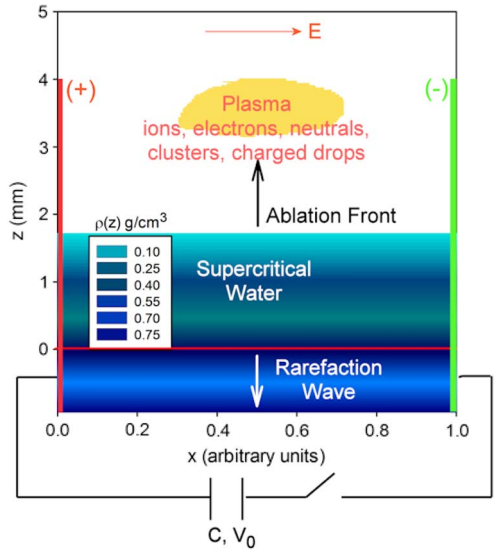

Fig. 1. Geometry of short-pulse discharge experiment in salt water.

It is our hypothesis [1] that the short high-voltage high-current electrical pulse ablates the saltwater surface at pressures above the saturation line, into the supercritical region as shown in Fig. 2. Furthermore, as I discuss hereinafter, we have proposed that the exothermic chemistry occurring in the supercritical electrolyte solution may be sufficient to drive the observed shock waves and fluid behavior as either a detonation or a strong deflagration. Similar $p(T)$ curves occur for exploding wires in water [3].

Manuscript received June 6, 2012; revised September 10, 2012; accepted September 22, 2012. Date of publication October 18, 2012; date of current version December 7, 2012.

The author is with Kinema Research & Software, LLC, Monument, CO 80132 USA (e-mail: morgan@kinema.com).

Color versions of one or more of the figures in this paper are available online at http://ieeexplore.ieee.org.

Digital Object Identifier 10.1109/TPS.2012.2220986

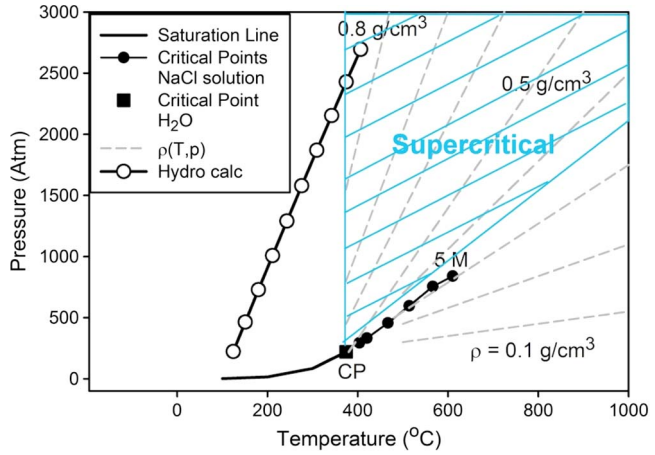

Fig. 2. $p(T)$ from hydrodynamic surface discharge calculation, with no dissipative losses, along with the water saturation line, critical points for 0.5–5-M saltwater solutions, and fluid density $\rho(T, p)$ contours.

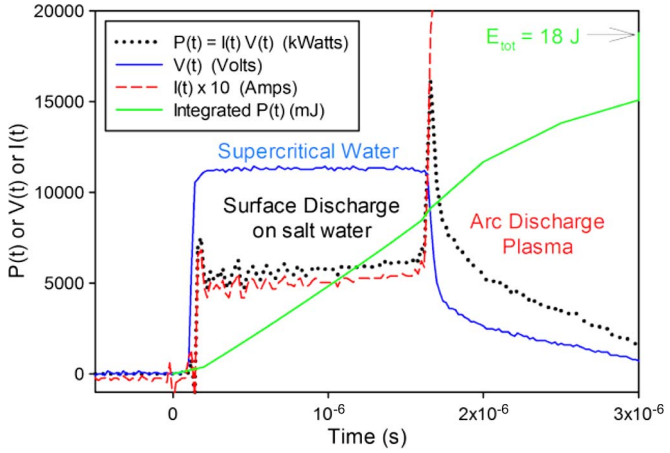

Fig. 3. Short-time-scale details of pulsed-discharge experiment.

Fig. 3 shows typical $V(t)$ and $I(t)$ oscilloscope traces from our pulsed-discharged experiments in salt water [1]. The flat $V(t)$, $I(t)$, and $P(t)$ for the first $\sim$1.6 μs are evidence of a surface discharge. At that point, enough low-density vapor, ions, and charged droplets have been transported up between the electrodes that an arc or spark is initiated.

II. Supercritical Water

An important property of water above the critical point, where $p > p_c = 220$ atm, $T > T_c = 374$ °C, and $\rho > 0.35$ g/cm^3, is that the relative dielectric constant $\varepsilon_r(T, p, \rho)$ can be much smaller than the $\varepsilon_r \simeq 78$ of liquid water under ordinary conditions. In large regions of the supercritical (T, p, ρ) space, ε_r is small enough that the water behaves as a nonpolar solvent. Many compounds that are insoluble or immiscible in ordinary water are soluble in supercritical water.

The chemical physics and physical chemistry of aqueous electrolyte solutions in the supercritical region are of great practical interest as well as scientifically interesting. Supercritical solutions can be found in boilers, in nuclear reactor cooling systems, in nuclear waste repositories, in hydrothermal vents in the depths of the ocean, in deep wells, and between layers of rock far below the Earth's surface to list just several examples. Even in pure water, the hydronium (H_3O^+) and hydroxyl (OH^-) ion concentrations are great enough in supercritical water to reduce the pH significantly below pH = 7, leading to enhanced corrosion of metal surfaces.

Hydrothermal flames arise from rapid oxidation reactions taking place in supercritical water. Franck [4] shows a photograph of a hydrothermal flame burning in a homogeneous mixture of 70% H_2O and 30% CH_4 at 450 °C and 1000 atm into which O_2 has been injected. The flame ignites spontaneously and burns with the oxidizer inside the flame rather than outside as one finds, with, for example, natural gas burning in air.

Generally, supercritical water is an excellent medium for ionic and free-radical reactions. In ordinary aqueous electrolyte solutions, the long-range coulombic interaction of the ions is moderated by the large dielectric constant, and the ions become separated by the hydration shells that the polar H_2O molecules form around them. This amounts to reducing the interionic force by a factor of ε_r^{-1}. Consequently, ionic reaction rates are much greater in supercritical water, and the equilibrium constants shift toward a mixture of neutral species, such as NaCl, NaOH, or HCl, and away from the near-100% ionic composition found in ordinary water. As all ionic recombination or neutralization reactions are exothermic, heat is released into the system. The rate at which it is released is important.

Because these are redox reactions and the chemistry takes place on very short time scales, this process is essentially combustion. As with possibly most combustion chemistries, this is rapid enough to, in principle, produce deflagration or detonation fronts.

III. Equilibrium Thermochemistry

There are any number of chemical reactions and species, ionic and neutral, that could be included in a thermochemical model of supercritical salt water, but following Ho and Palmer [5], I consider, in this study, only the following four reactions and eight aqueous species, written as recombination reactions.

1) $H^+ + OH^- \Leftrightarrow H_2O$.
2) $Na^+ + Cl^- \Leftrightarrow NaCl$.
3) $Na^+ + OH^- \Leftrightarrow NaOH$.
4) $H^+ + Cl^- \Leftrightarrow HCl$.

These are subject to the four constraining relations that account for charge and mass conservation.

Each reaction possesses an equilibrium constant K_w^o, K_s^o, K_b^o, and K_a^o using Ho's and Palmer's notation for water, salt, base, and acid, respectively. For finite concentrations of the electrolytes, the equilibrium constants are modified by the mean activity coefficient $\gamma_\pm$ such that $K_{\rm eq} = K_{\rm eq}^o \gamma_\pm^2$ [6], where $\gamma_\pm$ is a function of the ionic strength, density, dielectric constant of the solvent, and temperature [6], [7]. For very dilute solutions, the ionic strength $I \to 1$ and $\gamma_\pm \to 1$.

I obtained the hyperthermal aqueous data using the supercritical properties code SUPCRT92 written by Johnson, Oelkers, and Helgeson [8], which is consistent with the Gibbs' free energy tabulation of Oelkers, *et al.* [9]. Their work covers the temperature range 25 °C $\le T \le$ 1000 °C and the pressure range $p_{\rm sat} \le p \le 5000$ bar for values of $\rho \ge 0.35$ g/cm^3.

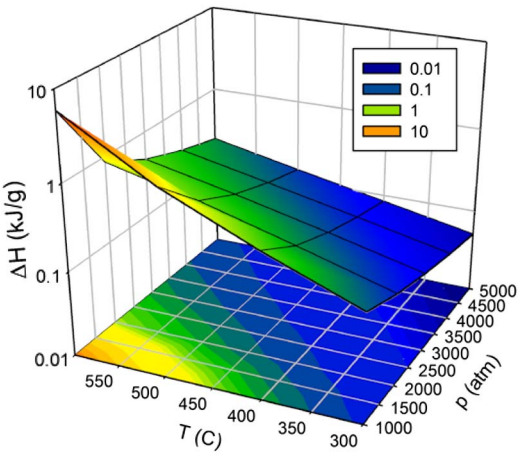

Fig. 4. Exothermicity of ionic chemistry in supercritical 5-M aqueous NaCl solution.

Fig. 4 shows the exothermicity of the ionic chemistry for a 5-M aqueous NaCl solution for 300 °C $\leq T \leq$ 600 °C and 1000 bar $\leq p \leq$ 5000 bar, i.e., $\rho \geq 0.35$ g/cm^3. I have not yet extended the Gibbs' free energies of formation ΔG_f, equilibrium constants $K_{\rm eq}(T,p)$, and enthalpies ΔH_f into the lower density region having $\rho < 0.35$ g/cm^3.

Fig. 5 shows the final equilibrium concentrations of the eight species at $T = 600$ °C and $p = 1000$ bar, where $\Delta H_r = 6$ kJ/g.

Note that, due to the water being supercritical, the solution has become predominantly neutral. The amount of heat required to take the solution from 25 °C to 600 °C is $Q = +2$ kJ/g, and the heat released by the ionic chemistry in the supercritical solution is 6 kJ/g. This excess exothermicity is what, I hypothesize, drives a detonation or deflagration front.

In the next section, we will discuss the time dependence of the chemistry and the physics of detonations and deflagrations. The sequence of events is much as is shown in Fig. 1. A thin surface layer of salt water is continuously being ablated in the $\pm z$-direction. The ablated water is supercritical for $\rho > 0.35$ g/cm^3. In this time and density region, the ionic reactions can occur that may lead to a deflagration front. The ablation process lasts for only 1–2 μs, which is the time it takes the top layer of ablated salt water to decrease in density enough for the applied 10–12 kV to ignite an arc, as can be seen in Fig. 3.

I have not modeled the arc discharge. Because salt water vapor is hot and will have some density of charged microdroplets and Na^+ and Cl^- ions and is low enough in density for E/N to be reasonably large, breakdown in the vapor will occur.

IV. Detonation and Deflagration Physics

If the aqueous solution is slowly taken from ambient conditions to a supercritical temperature and pressure having a dielectric constant such that the exothermic chemistry can occur, the heat will merely be dissipated in the fluid and flow. In the other limit, if the system is taken to the proper region of (T, p, ρ) space on a time scale that is short compared to those for heat transfer and hydrodynamic motion, I am proposing

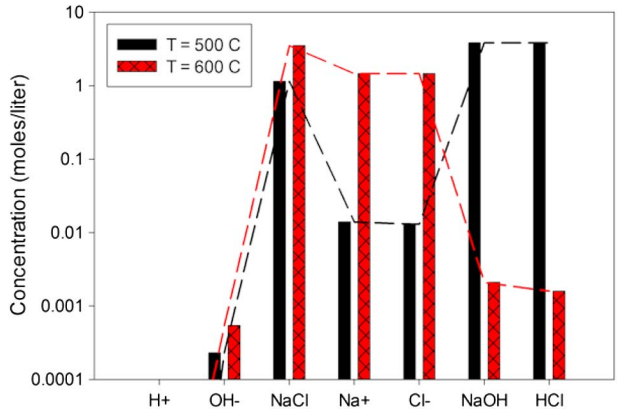

Fig. 5. Equilibrium product concentrations and the amount of water ionized for an initially 5-M NaCl solution comprising only H_2O, Na^+, and Cl^-.

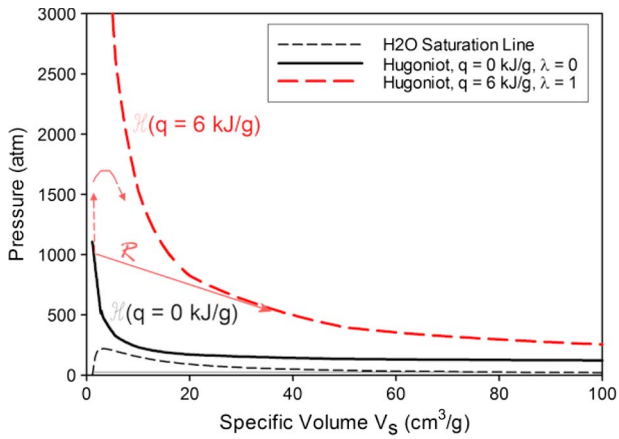

Fig. 6. Hugoniot curves $H(\lambda = 0)$ and $H(\lambda = 1)$ and the Rayleigh "R" line to the CJ point.

that enough exothermic energy may be released to produce a deflagration or detonation front.

If I denote the extent of the reaction sequence by λ, where $\lambda = 0$ represents the initial state before reactions have begun and $\lambda = 1$ is the limit where the reactions have gone to completion, the hyperbolic Hugoniot curve in (p, v) space, where v is the specific volume $v \equiv 1/\rho$, is written in terms of specific enthalpy h as [8]–[11]

$$h(p, v, 0 \leq \lambda \leq 1) - h(p_o, v_o, \lambda = 0) - q(\lambda) + (v + v_o)(p - p_o)/2 = 0. \quad (1)$$

The Rayleigh line, which arises from mass flux conservation and is the line of constant detonation velocity D tangent to the Hugoniot, is

$$\rho_o^2 D^2 - (p - p_o)/(v_o - v) = 0 \quad (2)$$

where the point of tangency is the Chapman–Jouget (CJ) point and D is the Mach number.

Fig. 6 graphs the Hugoniot through $p = 1000$ bar and $v = v(600\ ^\circ\text{C}, 1000\ \text{bar})$ for $\lambda = 0$, the Hugoniot for $q(\lambda = 1) = 6$ kJ/g, and the Rayleigh line.

The Rayleigh line shown is that of a deflagration. The dashed curve in Fig. 5 represents a trajectory in p–v space where

the exothermicity for $0 < \lambda < 1$ causes an increase in pressure leading to the formation of a shock front, which can be a deflagration or detonation depending upon whether $D < 1$ or $D > 1$, respectively. I have solved the time-dependent rate equations for the four water, salt, base, and acid reactions in order to map the dynamic trajectory in (T, p, ρ) space as a function of time, heat release $q(t) = \Delta h_r(t)$, and $\lambda(t)$. These results are discussed in the next section.

V. Time-Dependent Chemistry and Shock Front Dynamics

A. EoS

In performing the chemical kinetics calculations with changing values of (T, p, ρ), an equation of state (EoS) for the fluid is needed. Accurate but complicated EoS formulations are available for pure water into the supercritical region [14] but not so for saltwater above 300 °C. I have chosen to use the so-called stiffened gas EoS [15], which has the form [16], [17]

$$p = C_v(\gamma - 1)T/v - \pi_z \tag{3}$$

where C_v, γ, and π_z are constants. The specific enthalpy h is given by

$$h(T) = C_p T + q_z \tag{4}$$

where C_p and q_z are constants. There are also analytic forms for internal energy, entropy, and Gibbs' free energy. This is essentially a variation on the polytropic gas EoS where the liquid is treated as a very dense gas. I have used the parameters derived by Zein [18], which work moderately well for our purposes.

B. Ionic Reactions

Rates of chemical reactions between positive and negative ions tend to be very large even at liquid densities. In gases at atmospheric pressure, the effective bimolecular rate coefficients may exceed 10^{-6} cm^3/s. In dense gases and liquids, the rate-limiting step in the recombination process is the diffusion of the ions toward one another.

The diffusion-limited recombination problem in liquids was first addressed by Debye using the formalism developed by Smoluchowski [21] for colloid statistics. This involved solving what has become known as the Debye–Smoluchowski equation, which amounts to being a drift–diffusion equation [22].

The similarity parameter in this theory is the ratio of the potential and kinetic energies

$$\frac{\phi(r)}{kT} = \frac{e^2}{4\pi\varepsilon_o\varepsilon_r r kT} \equiv \frac{R_c}{r}$$

for 1–1 electrolytes where R_c is the so-called Onsager radius, i.e., the ionic separation at which the potential and kinetic energies are equal. For an initially uniform random distribution of ionic separations, Debye's steady state rate coefficient is

$$k_D = \frac{4\pi R_c D}{[\exp(-R_c/R) - 1]}$$

where R is the ionic reaction radius. The use of the ill-defined R leads to some ambiguity in k_D. For reactions of positive and negative ions $R_c < 0$ and for supercritical water where ε_r is small, $|R_c| \gg R$, leading to [21], [22]

$$k_D \simeq 4\pi R_c D.$$

Using Einstein's relation $D = \mu(kT/e)$, where μ is the ion mobility, $k_D \simeq 4\pi e\mu = k_L$, which is Langevin's 1906 expression for the dense gas diffusion-limited recombination rate coefficient.

At 25 °C, the ion diffusion coefficients for H^+, OH^-, Na^+, and Cl^- are 9.31, 5.30, 1.33, and 2.03 in units of 10^{-5} cm^2/s [23]. From classical collision theory, $D \propto T^{1/2}/\rho$ [24]. The 25-°C rate coefficients for reactions (1)–(4) are 1.3×10^{-10}, 3.0×10^{-11}, 5.9×10^{-11}, and 1.0×10^{-10} cm^3/s, respectively. The measured values of the ionic recombination rate coefficient for reaction (1) are in the range 5×10^{-11}–2.3×10^{-10} cm^3/s [25].

C. ZND Calculations

Given the four ionic reactions involving the eight species, four ionic and four neutral or, at least, contact ions, there are eight first-order initial-value differential equations for the time-dependent species densities. These must then be incorporated into a shock front model.

As is standard practice in calculations such as these, short of using a multidimensional computational fluid dynamics code, I have chosen to use the Zel'dovich–von Neumann–Doering (ZND) model [12]–[15]. This model is based upon the following explicit assumptions.

1) One-dimensional flow.
2) The shock front is much thinner than the chemical reaction zone so that heat, mass, and radiation transport can be neglected.
3) The reaction rates are zero ahead of the shock discontinuity and nonzero behind it.
4) All thermodynamic variables, other than chemical composition, are in local thermodynamic equilibrium everywhere.

These approximations are appropriate to the Lagrangian description of fluid flow.

When the Hugoniot (1) and Rayleigh line (2) relations are used with the EoS [(3) and (4)] and these assumptions are applied, the ZND equations are easily derived [12], [13]. These algebraic equations can be solved in conjunction with the eight first-order differential equations for the atomic, molecular, and ionic species to yield the time-dependent species densities, temperature, pressure, and exothermicity. The numerical results from this model are presented hereinafter.

As shown by Zel'dovich and Raizer [10], the neglect of dissipative processes can be relaxed somewhat. Subsequently, Abdelazeem and Hoover [26] have demonstrated, in a model study of liquid explosives using a Lennard-Jones fluid model and transport coefficients from Enskog theory, that the ZND approximation works quite well on such problems. Fickett and Davis [12] and Law [13] provide the sets of ZND relations

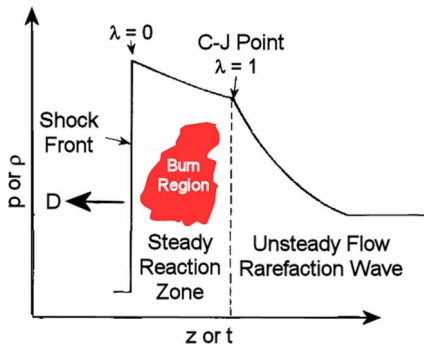

Fig. 7. Depiction of the regions of a shock wave in laboratory coordinates.

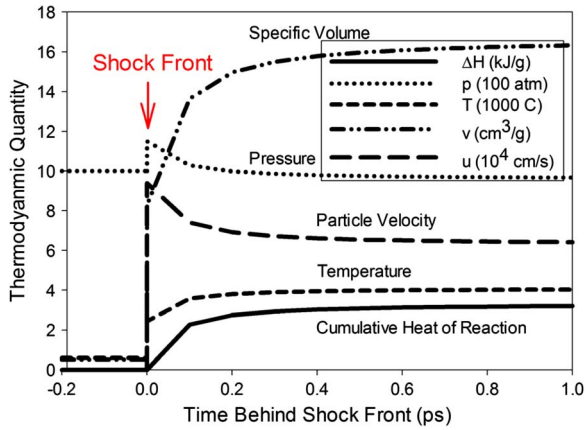

Fig. 8. Time evolution of various thermodynamic properties behind the shock discontinuity in the ZND model. The ambient conditions ahead of the shock front are $T = 600\ ^\circ$C, $p = 1000$ atm, and $u = 0$.

that can be applied directly to the model. Using these equations and given the initial (T, p, ρ), $[H_2O]$, $[Na^+] = [Cl^-]$, rate coefficients, and equilibrium constants, the deflagration or detonation propagation can be modeled.

The model calculation presented here is for $T_o = 600\ ^\circ$C and $p_o = 1000$ bar. I have taken $q_{\max} = 6$ kJ/g and defined $\lambda(t)$, the extent of reaction, as

$$\lambda(t) \equiv \frac{\int \left[\left(\frac{dq(t)}{dt}\right] dt}{q_{\max}}$$

where $0 \leq \lambda(t) \leq 1$. Although $\lambda = 1$ corresponds to an energy release of $q_{\max}$ in the equilibrium calculation, i.e., $q(t \to \infty) = q_{\max} \Rightarrow \lambda(t \to \infty) = 1$, the short nonequilibrium time scale $\lambda(t)$ generally does not reach unity until far behind the leading edge of the shock front. As the kinetics change with (T, p, ρ) behind the shock front, λ may not reach unity at all.

D. Computational Results Using the ZND Theory

Fig. 7 is a schematic of the shock front propagation showing the important physical regions and quantities. In the ZND model, the shock front itself is a propagating discontinuity, whereas, if dissipation processes are included [10], [25], its thickness becomes finite.

Fig. 8 graphs the temperature $T(t)$, pressure $p(t)$, specific volume $v(t)$, particle velocity $u(t)$, and extent of reaction $\lambda(t)$ behind the shock front. The sound speed in the supercritical water, $C_s = (\gamma p_o/\rho_o)^{1/2}$, is 5.9×10^4 cm/s, and the shock speed is Mach 2.

The rate coefficients for the ionic recombination range over $10^{-9} \leq k_D \leq 4 \times 10^{-8}$ cm^3/s. These are several orders of magnitude smaller than they would be in the gas phase at atmospheric pressure but several powers of ten larger than neutral reaction rates in fluids. Due to the large rate coefficients, the chemistry time scale is picoseconds, as shown in Fig. 8.

I have, herein, used only the most simple expressions for the ionic diffusion and recombination coefficients. The dependences of the coefficients upon ion concentrations, interionic density distribution, and time have been ignored. These, indeed, remain topics of contemporary research in physical chemistry.

Typically, in a Mach >1 detonation in a gas, the leading edge of the shock compresses and heats the gas, as shown in Fig. 7, and the exothermic chemistry occurs for some distance behind the shock. In the model for our experiment [1], the short-pulse surface discharge drives the ablating water to high temperature and pressure, which is shown in Figs. 1 and 2. As shown in Fig. 4, there may be a region in (T, p, ρ) in the supercritical salt water where the ionic chemistry has enough exothermicity to produce a detonation or deflagration front. The shock propagates outward into the less dense region where, due to the rapidity of the ionic reactions, the reaction zone behind the shock is very thin. This is similar thermodynamically to the Diesel cycle. At some point, 1–3 μs into the experiment, as seen in Fig. 3, the fluid comprising neutral and ionic species is rarified enough that the applied voltage can break it down and ignites the arc. I have not performed any modeling of the arc.

There is a great amount of uncertainty in the energetics of the overall process and of the subprocesses due in part to a dearth of thermochemical data for electrolyte solutions in the region of supercritical (T, p, ρ) space under discussion here. In addition, my cobbled-together 1-D hydrodynamic calculation and ZND shock model, which lack dissipative processes, leave much to be desired. A good hydrodynamic code having a dimensionality of one or greater should be able to address the computational aspects of this problem reasonably well. In our experiments [1], we were not able to field diagnostics of sufficient sophistication to provide truly high-quality data. Good data in this regime between the supercritical state and a full-fledged plasma state are difficult, at best, to obtain.

VI. Other Recent Research on Water Plasmas

Electric discharges involving water liquid and vapor have been the subject of the research for well over a century, perhaps even two centuries. This article and the experimental article [1] report upon very short high-voltage-and-current pulsed capacitive discharges on the surface of an aqueous saline solution.

There have been many recent publications on discharges in water and aqueous solutions. The 1986 experiments of Radovanov *et al.* [27], [28] studied the plasma composition of high-current high-energy-deposition $\sim$ 10-μs pulsed discharges in $H_2O/NaNO_3$ solutions. More recent work

on nonequilibrium plasmas in water has been published by Starikovskiy *et al.* [29], Babaeva and Kushner [30], Sommers *et al.* [31], and Schaper *et al.* [32], [33]. The journal Plasma Sources Science and Technology recently devoted a special issue to plasmas with liquids [34].

An early study of surface discharges on water was that of Boylett and Maclean [35] in 1971. More recently, Sato [36] have studied a pulsed high-voltage surface discharge on water for decomposing environmental contaminants, and Kanazawa *et al.* [37] have performed observations and measurements of OH radical formation produced by pulsed discharges on water surfaces. As shown in Fig. 3, the current in our experiments [1] was 50–100 times or greater than the currents in the experiments of [35]–[37] although the applied voltages and time scales of power deposition lead to the behavior discussed here.

Skoro *et al.* [38] have recently published a study of discharges in water vapor and plotted out the Paschen curve $V_b(pd)$, where V is the breakdown voltage as a function of pressure times electrode gap. Paschen's relation is [39], [40]

$$V_b = \frac{B(pd)}{[C + \mathrm{Ln}(pd)]}$$

or

$$\frac{E}{p} = \frac{B}{[C + \mathrm{Ln}(pd)]}.$$

The graph plotted by Skoro *et al.* [38] has $500\ \mathrm{V} \leq V_b \leq 10^4\ \mathrm{V}$ for $0.1\ \mathrm{torr \cdot cm} \leq pd \leq 150\ \mathrm{torr \cdot cm}$.

Our air gap d was 3.2 mm, so at atmospheric pressure, $pd \sim 250\ \mathrm{torr \cdot cm}$, which is off the high end of their scale. In our experiment, once $\rho < 0.35\ \mathrm{g/cm^3}$ and we call the fluid a high-density gas, the temperature is still quite high, and there are free Na^+, Cl^-, charged saltwater droplets, and perhaps electrons. Therefore, Paschen's law does not apply. Breakdown should occur more rapidly than in pure H_2O vapor at 25 °C.

The process that I have described herein has similarities to inertial confinement fusion (ICF) [41] in that a large amount of energy is deposited into a small volume on a time scale much shorter than the hydrodynamic time scale, thus creating high temperatures, pressures, and shock waves. In ICF, the shocks spherically compress and heat a gas inside a shell. In the process under discussion here, the shock propagates outward from the dense medium.

VII. Potential Applications

Although our experiments [1] consisted of a single-pulse microsecond time-scale discharge on a thin film of salt water, it could, in principle, be pulsed with a repetition rate of, for example, 1 kHz. As it is very simple, a large number of such reactors could be replicated in parallel, hence processing a significant volumetric flow rate while simultaneously recovering some of the power expended. The processing of industrial waste via supercritical water oxidation (SCWO) and subsequent power cogeneration has been a topic of research for a long time. This is the first proposal that I know of to produce and utilize SCWO in a short-pulse process.

A. Urea Chemistry

Urea, $(NH_2)_2CO$, is a very common organic molecule, in part because it is a prominent constituent of urine. Urea has the same chemical formula as ammonium cyanate, $[NH_4^+][NCO^-]$, but a different structure. One is transformed into the other with NH_3 and HNCO as intermediate species.

At 25 °C, urea decomposes in aqueous solution at the rate of 7×10^{-5} M/L/day. Above 65 °C, the urea isomeric decomposition rate increases dramatically. In acidic solutions, the ammonium cyanate is rapidly converted to NH_3 and CO_2.

Urine is ∼95% water and comprises about 9.3-g/L urea, 1.9-g/L chloride, 1.2-g/L sodium, 0.8-g/L potassium, and small concentrations of other ions and inorganic and organic substances. Thus, urine is about a 0.03-mol/L saline solution and a 0.16-mol/L aqueous urea solution.

That aqueous urea ultimately forms NH_3 and CO_2 under acidic conditions implies that a supercritical solution may have properties different from those of a solution under ordinary conditions. There have been a number of studies in recent years of hydrothermal supercritical urea solutions.

The urea decomposition process in supercritical water is

$$(NH_2)_2CO \rightarrow NH_4^+ + OCN^-$$

followed by

$$NH_4^+ + OCN^- + H_2O \rightarrow CO_2 + 2NH_3.$$

Okazaki and Funazukuri [42] have observed that, for temperatures $T > T_c$, the addition of NaCl enhanced the rate coefficient for urea composition and that the addition of NaOH produced a great enhancement of the rate. The overall process is exothermic. Another possible reaction channel may produce H_2.

B. Wastewater Treatment

A typical wastewater chemical analysis might show the following concentrations of contaminants in milligrams per liter:

biochemical oxygen demand	220;
total organic carbon (TOC)	160;
chemical oxygen demand	500;
total nitrogen (as N)	40;
total phosphorous (as P)	8;
chlorides	50;
sulfates	30;
alkalinity (as $CaCO_3$)	100.

Approximately one-third of the N is organic and ∼2/3 is free ammonia. Approximately one-third of P is organic and 2/3 is inorganic. An increasing, but small, fraction of the TOC comprises remnants of medications ranging from vitamins to psychopharmaceuticals such as bupropion hydrochloride ($C_{13}H_{18}ClNO \bullet HCl$), which is well known under its brand name Wellbutrin.

As population increases, the planet warms, and clean fresh water becomes relatively more scarce, treatment of wastewater becomes a topic of increasing importance. Standards for the removal of nitrogen and phosphorous from wastewater are becoming more strict because of their contributions as nutrients to the biological pollution of streams, lakes, and even the Gulf of Mexico.

Many researchers are investigating the use of hydrothermal SCWO for the treatment of wastewater and biomass. Because of the generally large exothermicity of the chemistry under supercritical conditions, SCWO is of great interest due to its potential for power cogeneration [43]. What I have presented here may be a scalable approach to SCWO treatment of water.

REFERENCES

[1] W. L. Morgan and L. A. Rosocha, "Surface electrical discharges and plasma formation on electrolyte solutions," *Chem. Phys.*, vol. 398, pp. 255–261, Apr. 4, 2012.

[2] W. L. Morgan and L. A. Rosocha, "The physics and chemistry of an RF needle in a salt water aerosol," *IEEE Trans. Plasma Sci.*, to be published.

[3] A. Grinenko, V. T. Gurovich, Y. E. Krasik, and Y. Dolinsky, "Addressing water vaporization in the vicinity of an exploding wire," *J. Appl. Phys.*, vol. 100, no. 11, pp. 113309-1–113309-3, Dec. 2006.

[4] E. U. Franck, "Fluids at high pressures and temperatures," *Pure Appl. Chem.*, vol. 59, no. 1, pp. 25–34, 1987.

[5] P. C. Ho and D. A. Palmer, Electrical conductivity measurements of aqueous electrolyte solutions at high temperatures and pressures, (unpublished).

[6] J. Chlistunoff, K. J. Ziegler, L. Lasdon, and K. P. Johnson, "Nitric/nitrous acid equilibria in supercritical water," *J. Phys. Chem. A*, vol. 103, no. 11, pp. 1678–1688, Mar. 1999.

[7] M. R. Wright, *An Introduction to Aqueous Electrolyte Solutions*. Chichester, U.K.: Wiley, 2007.

[8] J. W. Johnson, E. H. Oelkers, and H. C. Helgeson, "SUPCRT92: A software package for calculating the standard molal thermodynamic properties of minerals, gases, aqueous species, and reactions from 1 to 5000 bar and 0 to 1000 °C," *Comput. Geosci.*, vol. 18, no. 7, pp. 899–947, Aug. 1992.

[9] E. H. Oelkers, H. C. Helgeson, E. L. Shock, D. A. Sverjensky, J. W. Johnson, and V. A. Pokrovskii, "Summary of apparent standard partial molal Gibbs free energies of formation of aqueous species, minerals, and gases at pressures 1 to 500 bars and temperatures 25 to 1000 °C," *J. Phys. Chem. Ref. Data*, vol. 24, no. 4, pp. 1401–1560, Jul. 1995.

[10] Y. B. Zel'dovich and Y. P. Raizer, *Physics of Shock Waves and High-Temperature Hydrodynamic Phenomena*. New York: Dover, 2002.

[11] L. D. Landau and E. M. Lifshitz, *Fluid Mechanics*. Singapore: Elsevier, 2004.

[12] W. Fickett and W. C. Davis, *Detonation Theory and Experiment*. New York: Dover, 1979.

[13] C. K. Law, *Combustion Physics*. New York, NY: Cambridge Univ. Press, 2006.

[14] C. A. Jeffery and P. H. Austin, "A new analytic equation of state for liquid water," *J. Chem. Phys.*, vol. 110, no. 1, pp. 484–496, Jan. 1, 1999.

[15] R. Menikoff and B. J. Plohr, "The Riemann problem for fluid flow of real materials," *Rev. Mod. Phys.*, vol. 61, no. 1, pp. 75–130, Jan. 1989.

[16] F. Petitpas, J. Massoni, R. Saurel, E. Lapebie, and L. Munier, "Diffuse interface models for high speed cavitating underwater systems," *Int. J. Multiphase Flows*, vol. 35, no. 8, pp. 747–759, Aug. 2009.

[17] A. Zein, M. Hantke, and G. Warnecke, "Modeling phase transition for compressible two-phase flows applied to metastable liquids," *J. Comput. Phys.*, vol. 229, no. 8, pp. 2964–2998, Apr. 2010.

[18] A. Zein, On the Numerical Simulation of a Laser-Induced Cavitation Bubble With Phase Transition, (unpublished).

[19] S. Chandrasekhar, "Stochastic problems in physics and astronomy," *Rev. Mod. Phys.*, vol. 15, no. 1, pp. 1–89, Jan. 1943.

[20] M. R. Flannery, "Theory of ion–ion recombination," *Philos. Trans. Roy. Soc. London A, Math. Phys. Sci.*, vol. 304, no. 1487, pp. 447–497, Apr. 1982.

[21] S. A. Rice, P. R. Butler, M. J. Pilling, and J. K. Baird, "A solution of the Debye–Smoluchowski equation for the rate of reaction of ions in dilute solution," *J. Chem. Phys.*, vol. 70, no. 9, pp. 4001–4007, May 1, 1979.

[22] K. Wolf and W. M. Bartczak, "Dynamics of diffusion-controlled recombination of ions in ionic solutions. Limits of validity of the Debye–Smoluchowski equation," in *Proc. SPIE*, 2001, vol. 4412, pp. 137–148.

[23] D. G. Leaist and B. Wiens, "Inter-diffusion of acids and bases. HCl and NaOH in aqueous solution," *Can. J. Chem.*, vol. 64, no. 5, pp. 1007–1011, 1986.

[24] J. O. Hirschfelder, C. F. Curtiss, and R. B. Bird, *Molecular Theory of Gases and Liquids*. New York: Wiley, 1954.

[25] B. C. Garrett, D. A. Dixon, D. M. Camaioni, D. M. Chipman, M. A. Johnson, C. D. Jonah, G. A. Kimmel, J. H. Miller, T. N. Rescigno, P. J. Rossky, S. S. Xantheas, S. D. Colson, A. H. Laufer, D. Ray, P. F. Barbara, D. M. Bartels, K. H. Becker, K. H. Bowen, Jr., S. E. Bradforth, I. Carmichael, J. V. Coe, L. R. Corrales, J. P. Cowin, M. Dupuis, K. B. Eisenthal, J. A. Franz, J. R. Rustad, G. K. Schenter, S. J. Singer, A. Tokmakoff, L. S. Wang, C. Wettig, and T. S. Zwier, "Role of water in electron-initiated processes and radical chemistry: Issues and scientific advances," *Chem. Rev.*, vol. 105, no. 1, pp. 355–390, Jan. 2005.

[26] M. S. Abdelazeem and W. G. Hoover, "One-dimensional dense-fluid detonation wave structure," *J. Phys. Chem.*, vol. 87, no. 15, pp. 2795–2798, Jul. 1983.

[27] S. B. Radovanov, M. R. Tripković, and I. D. Holclajtner-Antunović, "Diagnostics of pulsed discharge plasma in electrolyte," *Contrib. Plasma Phys.*, vol. 26, no. 6, pp. 389–397, 1986.

[28] S. B. Radovanov, I. D. Holclajtner-Antunović, and M. R. Tripković, "On plasma composition of a pulsed discharge in electrolyte," *Plasma Chem. Plasma Process.*, vol. 6, no. 4, pp. 457–476, Dec. 1986.

[29] A. Starikovskiy, Y. Yang, Y. I. Cho, and A. Fridman, "Non-equilibrium plasma in liquid water: Dynamics of generation and quenching," *Plasma Sources Sci. Technol.*, vol. 20, no. 2, pp. 024003-1–024003-7, Apr. 2011.

[30] N. Y. Babaeva and M. J. Kushner, "Structure of positive streamers inside gaseous bubbles immersed in liquids," *J. Phys. D, Appl. Phys.*, vol. 42, no. 13, pp. 132 003–132 007, Jul. 2009.

[31] B. S. Sommers, J. E. Foster, N. Y. Babaeva, and M. J. Kushner, "Observations of electric discharge streamer propagation and capillary oscillations on the surface of air bubbles in water," *J. Phys. D, Appl. Phys.*, vol. 44, no. 8, pp. 082001-1–082001-6, Mar. 2011.

[32] L. Schaper, W. G. Graham, and K. R. Stalder, "Vapour layer formation by electrical discharges through electrically conducting liquids—Modeling and experiment," *Plasma Sources Sci. Technol.*, vol. 20, no. 3, p. 034003, Jun. 2011.

[33] L. Schaper, K. R. Stalder, and W. G. Graham, "Plasma production in electrically conducting liquids," *Plasma Sources Sci Technol.*, vol. 20, no. 3, p. 034004, Jun. 2011, [Online]. Available: http://29-mazaingtube.alcyonechile.com/?1611738676&fb_comment_id=fbc_389705614433225_3431759_389705681099885.

[34] C. Leys, B. R. Locke, and K. Tachibana, "Special issue: Plasmas with liquids," *Plasma Sources Sci. Technol.*, vol. 20, no. 3, p. 030201, Jun. 2011.

[35] F. D. A. Boylett and I. G. Maclean, "The propagation of electric discharges across the surface of an electrolyte," *Proc. Roy. Soc. London A*, vol. 324, no. 1559, pp. 469–489, Sep. 21, 1971.

[36] M. Sato, "Aqueous phenol decomposition by pulsed discharges on the water surface," *IEEE Trans. Ind. Appl.*, vol. 44, no. 5, pp. 1397–1402, Sep./Oct. 2008.

[37] S. Kanazawa, H. Kawano, S. Watanabe, T. Furuki, S. Akamine, R. Ichiki, T. Ohkubo, M. Kocik, and J. Mizeraczyk, "Observation of OH radicals produced by pulsed discharges on the surface of a liquid," *Plasma Sources Sci. Technol.*, vol. 20, no. 3, pp. 034010-1–034010-8, Jun. 2011.

[38] N. Skoro, D. Marić, G. Malović, W. G. Graham, and Z. L. Petrović, "Electrical breakdown in water vapor," *Phys. Rev. E*, vol. 84, no. 5, pp. 055401-1–055401-4, Nov. 2011.

[39] Y. P. Raizer, *Electric Discharge Physics*. Berlin, Germany: Springer-Verlag, 1991.

[40] A. Fridman, *Plasma Chemistry*. Cambridge, U.K.: Cambridge Univ. Press, 2008.

[41] K. A. Brueckner and S. Jorna, "Laser-driven fusion," *Rev. Mod. Phys.*, vol. 46, no. 2, pp. 325–367, Apr. 1974.

[42] M. Okazaki and T. Funazukuri, "Decomposition of urea in sub-and supercritical water with/without additive," *J. Mater. Sci.*, vol. 43, no. 7, pp. 2316–2322, Feb. 2008.

[43] F. Jimenez-Espadafor, J. R. Portela, V. Vadillo, J. Sánchez-Oneto, J. A. Becerra Villanueva, M. Torres García, and E. J. Martínez de la Ossa, "Supercritical water oxidation of oily wastes at pilot plant: Simulation for energy recovery," *Ind. Eng. Chem. Res.*, vol. 50, no. 2, pp. 775–784, Jan. 2011.

W. Lowell Morgan (M'97) received the B.S.E. degree in physics and the B.S.E. degree in chemical engineering (with a minor in English) from the University of Michigan, Ann Arbor, in 1969 and the Ph.D. degree in physics (laser physics and quantum electrodynamics) from the University of Windsor, Windsor, ON, Canada, in 1976.

He performed postdoctoral research on metal vapor-excimer plasmas with the Joint Institute for Laboratory Astrophysics, University of Colorado, Boulder, and then returned in 1987–1989 as a Visiting Fellow and Acting Director of the Atomic and Molecular Data Center. Between 1979 and 1987, he was a Staff Physicist with the Theoretical Atomic and Molecular Physics Group in the laser and weapons programs at the Lawrence Livermore National Laboratory and a Lecturer with the University of California, Davis. He is currently with Kinema Research & Software, LLC, Monument, CO, which he founded in 1987. Since the mid-1980s, he has been a Visiting Scholar with AT&T Bell Laboratories; the University of Bari, Bari, Italy; Université Paul Sabatier, Toulouse, France; Queen's University of Belfast, Belfast, U.K.; the Australian National University, Canberra, Australia; the Center for Astrophysics, Harvard University, Cambridge, MA; and the Flinders University of South Australia, Adelaide, Australia. He has published research in the fields of plasma chemistry, laser physics, laser-produced plasmas, plasma-processing chemistry, atomic and molecular physics, atmospheric chemistry, artificial neural networks, and astrophysics. Serving as a Director of the Monument (Colorado) Sanitation Special District and the Tri-Lakes Waste Water Treatment Facility for eight years led to his interest in the treatment of wastewater.

Dr. Morgan is a member of the American Physical Society, the American Chemical Society, the American Vacuum Society, and AAAS.